NANO LETTERS

2007
Vol. 7, No. 6
1598−1602

Diameter-Dependent Elastic Modulus Supports the Metastable-Catalyst Growth of Carbon Nanotubes

Kyumin Lee,*,† Branimir Lukić,† Arnaud Magrez,† Jin Won Seo,†,‡ G. Andrew D. Briggs,§ Andrzej J. Kulik,† and László Forró*,†

Ecole Polytechnique Fédérale de Lausanne (EPFL), Institute of Physics of Complex Matter, 1015 Lausanne, Switzerland, and Department of Materials, Oxford University, Parks Road, Oxford OX1 3PH, Great Britain

Received March 2, 2007; Revised Manuscript Received April 25, 2007

ABSTRACT

We measured the elastic modulus of individual multiwalled carbon nanotubes (MWCNTs) grown by catalytic chemical vapor deposition (CVD) over a broad diameter range (10–25 nm). Alternating current (ac) dielectrophoresis was used for efficient tube deposition, and atomic force microscope (AFM) force–displacement curve technique was used for stiffness measurements. The elastic modulus exhibits a strong diameter dependence, showing a difference of nearly 2 orders of magnitude in the 10–20 nm diameter range (thinner MWCNTs have higher elastic modulus). Our results support the metastable-catalyst model in which the catalyst's molten skin plays a key role.

Chemical vapor deposition (CVD) is currently the most widespread method of producing carbon nanotubes (CNTs).[1] Its popularity is mainly due to the large-scale production feasible with appropriate facilities[2−5] and also the possibilities of controlling length, diameter, orientation, and growth sites.[6] To grow CNTs by CVD, metal nanoparticles (usually Fe, Ni, Co, or their alloys) are prepared on a support and they are subsequently exposed to a carbon-containing gas between 500 and 1500 °C. When conditions such as partial pressure and temperature are suitable, CNTs grow from the nanoparticles (catalysts). The typical product is the multiwalled carbon nanotubes (MWCNTs) that are 5−20 nm thick and a few to tens of micrometers long.

The vapor−liquid−solid (VLS) model[7] is frequently adopted to explain the CNT growth in CVD. Details of the catalytic CNT growth, however, are not clearly understood, and the exact role of the catalyst is a topic of intensive study.[8] One of the debated issues is whether the catalyst is solid or liquid during the CNT growth.[9] While the original VLS model assumes a liquid catalyst, CVD processes are typically carried out at temperatures well below both the bulk melting point and the eutectic temperature. The small size (typically 2−20 nm in diameter) may allow a catalyst to melt at these temperatures,[10] but predicting the exact physical state is difficult due to other factors: the shape, the carbon content,[11,12] the catalyst−support interface,[13,14] and the catalyst−nanotube interface.[15,16] For typical synthesis temperatures (700−1000 °C), all three states—completely liquid, partially liquid, and completely solid—may coexist due to a distribution in the catalyst size.

The liquid−solid state of a catalyst is important in determining the structure of the produced nanotube. Transmission electron microscopy (TEM) studies have reported that liquid catalysts favor tubular MWCNT growth, while solid catalysts lead to defective structures.[15,17−19] Bartsch and co-workers[18,19] notably reported that fast tubular growth from small catalysts dominated the early stage of CVD before eventually being outnumbered by slow bamboolike growth from larger catalysts. Given these observations, we expect a diameter dependence in the structural quality of MWCNTs grown from a CVD process—thinner nanotubes should show better structures—but it is difficult to quantify the structural quality of MWCNTs using TEM images.

A proven method for characterizing a CNT is to test its mechanical strength. Atomic force microscopy (AFM) and TEM studies have verified the ideal 1 TPa elastic modulus for arc-discharge-grown MWCNTs.[20−23] We had previously reported low elastic modulus (1−100 GPa) for CVD-grown MWCNTs[23,24] but afterward observed high elastic modulus values for double- to quadruple-walled CNT ropes grown by CVD.[25] While the bending modulus of the latter CNT ropes displayed the diameter dependence already observed for single-walled CNT (SWCNT) ropes (weak coupling between the constituent tubes leads to a very low shear

* Corresponding authors. E-mail: lee.kyumin@gmail.com (K.L.); laszlo.forro@epfl.ch (L.F.).
† EPFL.
‡ Current affiliation: Katholieke Universiteit Leuven, Belgium.
§ Oxford University.

10.1021/nl070502b CCC: $37.00 © 2007 American Chemical Society
Published on Web 05/16/2007

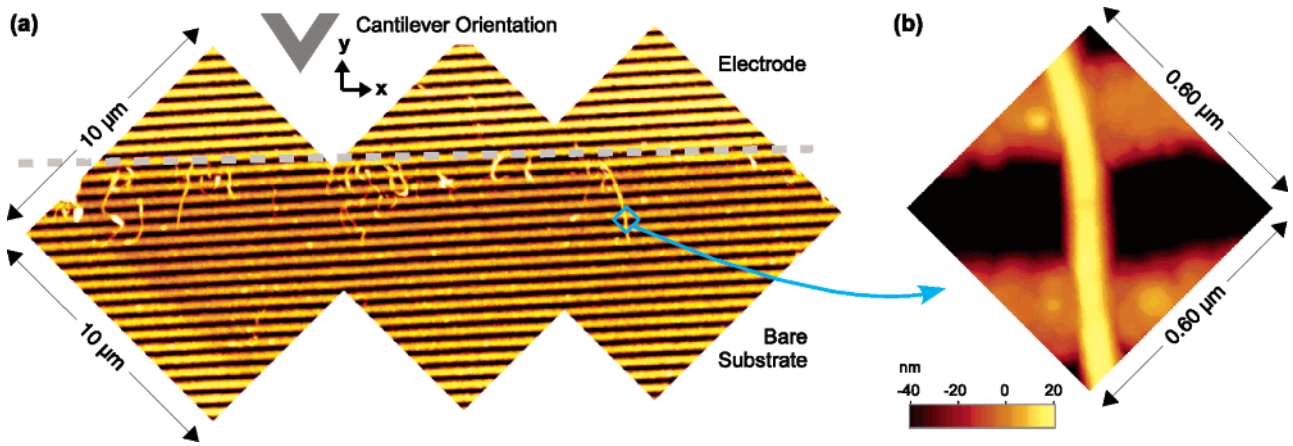

Figure 1. (a) MWCNTs deposited at an electrode boundary by ac dielectrophoresis. The opposing electrode is not visible at this scale. (b) A closeup AFM image of a suspended MWCNT.

modulus for the bundle),[26] the small-diameter (<5 nm) ropes, probably individual tubes, displayed the ideal 1 TPa stiffness. As our previous low-elastic-modulus results on CVD-grown MWCNTs were obtained from tubes of large diameter (>15 nm), the latter findings prompted us to investigate whether we can observe a diameter dependence in the elastic modulus if a proper diameter range is covered.

In this work, we report the elastic modulus measured for individual CVD-grown MWCNTs in the 10−25 nm diameter range. The elastic modulus shows a striking change in the 10−20 nm diameter range. The diameter dependence is good evidence for the metastable-catalyst growth model, discussed in detail later. We also describe an improved method of measuring the bending stiffness of CNTs.

Our experiment involves two steps: (1) depositing individual CNTs over holes or trenches and (2) deflecting the suspended structures with an AFM cantilever. CNTs were first dispersed in a solvent (ethanol or isopropanol) using an ultrasonic finger before deposition. Once deposited, the adhesion of a CNT on the flat parts of the substrate is often much stronger than the normal force applicable by the AFM cantilever,[23] so that we modeled the suspended nanotube as a doubly clamped beam.[27] We also assumed that the beam has a uniform and circular cross section. The midpoint of a doubly clamped beam deflects by δ when loaded with a force F, and the bending modulus E_b can be derived from the $F-\delta$ graph using the equation

$$E_b = \frac{L^3}{192I}\frac{dF}{d\delta} \quad (1)$$

where L is the suspended length and I is the second moment of area of the beam, which for a filled cylinder is $\pi D^4/64$. D is the outer diameter of the nanotube. We consider shear to be negligible for the suspended MWCNTs, as in the case of long thin beams, and take the bending modulus to be the elastic modulus E.[23] Both L and D are measured from the relevant AFM image and have typical uncertainties of ±10% and ±5%, respectively, which lead to a typical ±40% uncertainty in the calculated E value. The AFM cantilever stiffness is calibrated by noting the difference between actual and nominal cantilever resonance frequencies.

Two different methods were used for the stiffness ($dF/d\delta$) measurements. For some nanotubes, the method developed by J.-P. Salvetat[23] was used. CNT dispersion droplets were dried on a polished alumina ultrafiltration membrane, and a number of contact-mode AFM images were taken on a suspended nanotube using different feedback setpoints. We extracted a $F-\delta$ pair from each image and calculated the nanotube stiffness from the data plot. This method has two drawbacks: (1) random deposition makes finding a suitable nanotube a time-consuming process, and (2) the $F-\delta$ data is not detailed enough to analyze any irregularities that may arise during bending. To address these problems, we developed an improved method by adopting alternating current (ac) dielectrophoresis and force−displacement curves.

For CNT deposition by ac dielectrophoresis,[28] a GaAs wafer with 200 nm deep trenches microfabricated at 0.5 μm intervals was used as the substrate. Gold electrodes 30 nm thick with a 100 μm gap were prepared on the substrate by thermal evaporation. With an ac voltage (20 Vpp, 10 MHz) being applied between the two electrodes, a few droplets of nanotube dispersion were deposited at the gap and were left to dry. Figure 1 shows a typical result. As most of the nanotubes are deposited at the electrode boundaries, finding a suitable nanotube requires only a few AFM images.

To measure the stiffness of a suspended nanotube, we pushed down at its midpoint with an AFM cantilever, acquiring force−displacement[29] data during the loading and unloading processes. A typical loading curve is shown in Figure 2a. The $F-\delta$ curves were then obtained by subtracting a reference force−displacement curve taken on a flat substrate. Stiffness values were measured by fitting lines through these curves. The original Salvetat method and the improved method gave very close results on the same CNTs. By selecting the nanotubes lying nearly parallel to the cantilever's long axis, we minimized the effect of deflection-induced change in tip position.[30] AFM cantilevers with large tip radii (>50 nm) were used to avoid influences of thermal drifts. Furthermore, our AFM (Park Systems XE-100) has a

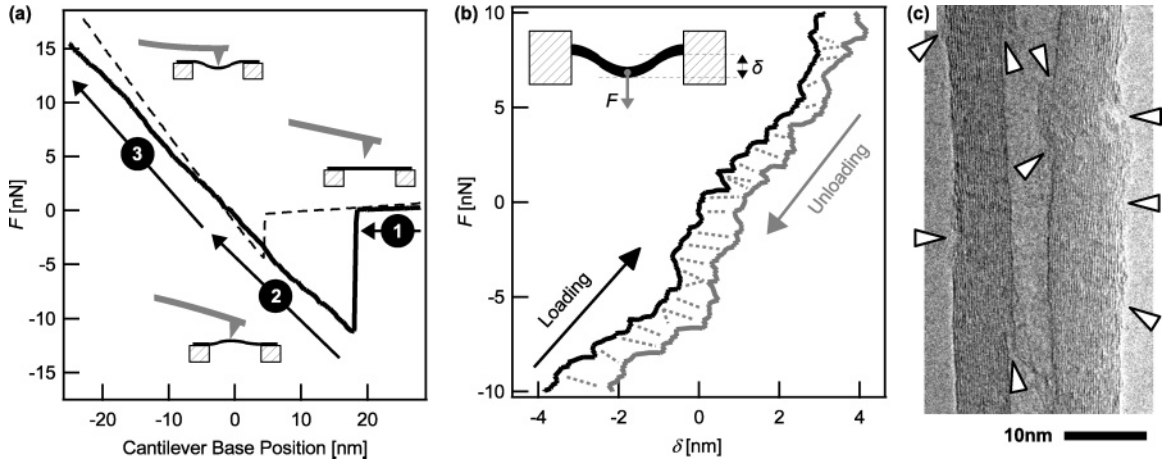

Figure 2. (a) In AFM force−displacement curve technique, the tip is first lowered into contact with the sample and then it is pulled off contact. Cantilever deflection (proportional to the loading force F) and cantilever base (z scanner) position are measured during the process. A loading curve on a suspended CNT (solid line) and that on a flat reference surface (dashed line) have different slopes due to the CNT deflection. (b) By comparing the loading and unloading curves on a CNT with those on a flat surface, a $F-\delta$ graph can be obtained. Some matching kinks in the loading and unloading curves are indicated by dashed lines. (c) TEM image of a CVD-grown MWCNT. Markers indicate structural defects.

2-D flexure scanner for the $x-y$ sample movement and a separate 1-D flexure scanner for the z probe movement, allowing cantilever (z scanner) motion orthogonal to the sample plane regardless of the $x-y$ scanner position.[31]

Figure 2b shows a typical pair of loading and unloading $F-\delta$ curves. The curves appear generally linear, confirming that the small deformation model behind eq 1 is still valid for our experiment. However, there are more details in the curves that were not available with the previous method. Numerous *kinks* are present, and we find matching pairs of kinks in the loading and the unloading curves. The kinks are not perfectly periodic, and some large kinks in a curve are divided into smaller kinks on the other curve. These clues hint that the kinks come from mechanical instabilities. As our AFM tip slips by roughly 10 nm along the nanotube (y-axis in Figure 1a) over a 20 nN loading range,[32] one may consider the atomic-scale stick−slip motion of AFM tip on graphite[33] as the source of these kinks. But the aperiodicity of the kinks is difficult to explain with this idea. In our opinion, the kinks are related to the motion of structural defects—coffee-cup structures, bamboo nodes, incomplete shells, etc.—present in a CVD-grown MWCNT (Figure 2c). When a nanotube bends, sliding and shearing would occur as a series of reversible stick−slip events at these defect sites, and such intrananotube dynamics would give rise to the observed kinks. They will be studied more in detail in a subsequent contribution.

Two batches of CVD-grown MWCNTs were used in this study: (1) MWCNTs produced in the temperature range of 700−800 °C using acetylene as a carbon precursor and Co nanoparticles as catalysts on a NaY zeolite support[34] and (2) MWCNTs obtained by heating a sample of the first batch to 2400 °C in a graphitization furnace. We had already reported that heat treatment could not improve MWCNTs' mechanical properties.[23,24] Nanotubes from both batches of similar diameter gave very close elastic modulus values, confirming that the two batches were equal in their mechanical properties. Altogether, 25 individual MWCNTs were analyzed. Study by TEM showed that nanotubes from the two batches in the 10−25 nm diameter range were individual MWCNTs and not ropes formed of thinner tubes. Also, we avoided any structure that diverged at its ends or changed significantly in diameter along its length when observed with AFM, thereby avoiding any bundle that may have formed during dispersion and deposition.

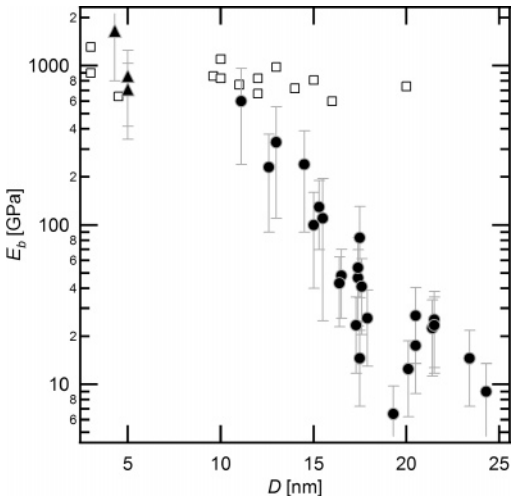

Figure 3. Circles: results on CVD-grown MWCNTs. Triangles: bending modulus of small-diameter CVD-grown double-walled CNT ropes.[25] Squares: nanotubes grown by arc-discharge evaporation.[23,26]

Figure 3 summarizes our results. The elastic modulus varies dramatically in the 10−20 nm diameter range, increasing almost exponentially with decreasing diameter. Data for small-diameter double- to quadruple-walled CNT ropes have been included to show the upper limit possible with CVD-grown MWCNTs (triangles in Figure 3).[25] Previous results on CNTs and small-diameter CNT ropes grown by arc-discharge evaporation are also included in the graph for comparison (squares in Figure 3).[23,26] Unlike the CVD-

grown MWCNTs, the arc-discharge-grown MWCNTs showed fairly constant elastic modulus over the same diameter range.

A number of theoretical works have actually predicted the CNT elastic modulus to drop with decreasing diameter because of the excessive strain imposed on the graphene shells at small diameters.[35,36] But the effect is important mostly for small-diameter SWCNTs (<1.5 nm), and we believe that it is not relevant to our results, as we are dealing with MWCNTs of larger diameters.

In contradiction to our previous arc-discharge data, Poncharal et al.[37] observed a diameter dependence in the effective modulus of individual arc-discharge-grown MWCNTs. In their work, they applied an ac electric field inside a TEM to drive a nanotube oscillation, and calculated the bending modulus from the frequency−amplitude data. They attributed the diameter dependence to the *rippling* of nanotube walls that was observed on some curved nanotubes. In our $F-\delta$ data, we did not find any transition from the linear small-deflection bending mode to a nonlinear ripple-bending mode. It is possible that the ripples were never introduced during our experiments due to lower curvatures. Furthermore, an alternative explanation for Poncharal's data has been offered by a recent molecular dynamics simulation.[38] In the cited work, Akita et al. showed intershell interactions in a vibrating double-walled nanotube to dissipate energy, and the simulated results agreed well with their experimental data. The proposed damping mechanism would be important for dynamic methods while not effecting our static methods. For these reasons, we believe that our diameter dependence was not caused by surface rippling of nanotubes.

Up to this point, we have neglected shear deformation. Shear should be negligible for long, thin beams composed of an isotropic material. This assumption should still hold for MWCNTs if the shells are continuous over the suspended length. Shearing a single nanotube shell is similar to shearing a graphene sheet in-plane, changing the angles between sp^2-hybridized orbitals of carbon. The shear modulus G for such deformation is 330 GPa,[26] high enough so that shear may be disregarded for MWCNTs with pristine shells. But CVD-grown MWCNTs often contain many defects, and a large number of incomplete shells exist. Because shearing a graphene sheet over a neighboring sheet is a relatively easy process ($G = 4.5$ GPa), intershell sliding between nanotube fragments (intrananotube stick−slip at defect sites, as mentioned earlier) would then dominate the bending deformation of a CVD-grown MWCNT. When shear deformation cannot be neglected, eq 1 may be rewritten to give the total deflection

$$\delta = \frac{FL^3}{192E_bI} = \frac{FL^3}{192EI} + f_s\frac{FL}{4GA} \tag{2}$$

where f_s is the shape factor (varying with the exact tube dimensions[39] but close to 1), and A is the cross-sectional area of the nanotube, at $\pi D^4/4$. After expanding I and A, we obtain

$$E_b = E\left(1 + 3f_s\frac{E}{G}\frac{D^2}{L^2}\right)^{-1} \tag{3}$$

If eq 3 fits well with our data for certain fixed values of E and G, the MWCNT quality may be argued to be diameter-independent, as the diameter dependence in bending modulus could stem purely from geometrical factors and the anisotropic nature of MWCNTs. But the strong, almost exponential, change of bending modulus in the 10−20 nm diameter range cannot be accounted for by the polynomial behavior of eq 3 nor by corrections to the coefficients to allow for a hollow core. Therefore, we conclude that the observed diameter dependence is a reflection of the diameter-dependent material quality: when grown in CVD, thinner MWCNTs are structurally superior to the thicker tubes.

The observed diameter dependence is a strong evidence for the metastable-catalyst growth model proposed by Kukovitsky and co-workers.[15,17] This model emphasizes the role of partially molten catalysts that have liquid *skins* covering solid cores.[10] The liquid skin, which may be metastable,[40] is extremely important because carbon diffusion would occur predominantly through this layer, and any instabilities at the layer would disturb the CNT growth.[41] In CVD, the catalyst is continuously agitated by exothermic precursor dissociation and endothermic carbon precipitation, the processes which may appear to the catalyst as discrete events on the time scale at which changes can occur to its liquid skin. Therefore, it is realistic to assume that instabilities *do* exist and that the catalyst−nanotube interface suffers from numerous perturbations during CNT growth. TEM movies of CNT growth in CVD (supporting information presented by Helveg et al.[42]) have shown catalysts undergoing numerous morphological changes.

Perturbations at the catalyst−nanotube interface would cause structural defects in the produced MWCNT, degrading its quality. The frequency and the gravity of perturbation would depend on the catalyst size. Under the same conditions, the smaller catalyst would have a thicker liquid skin due to its larger surface-to-volume ratio. The thicker skin would lead to a less frequent fluctuation at the nanotube−catalyst interface as well as allowing a more stable carbon diffusion despite some perturbations. So a MWCNT with a better structure would grow from the smaller catalyst. The observed *transition* in the elastic modulus over the 10−20 nm diameter range confirms this conclusion. Considering that 30 nm Co particles have been observed to melt at 600 ± 50 °C in methane atmosphere on silica support,[9] our 10−20 nm transition range is situated slightly lower than expectation. The difference could be due to a number of reasons: a catalyst often produces a MWCNT thinner than its size, and the carbon precursor and the support were different in our case. Nonetheless, the diameter-dependent variation of the elastic modulus is a strong evidence for the metastable-catalyst growth model.

In summary, we have measured the elastic modulus of individual MWCNTs grown from a single CVD process. The data show the elastic modulus changing dramatically in a narrow diameter range. The diameter dependence in elastic

modulus is a strong evidence for the metastable-catalyst growth of MWCNTs in CVD.

It is difficult to arrive at the near-exponential diameter dependence starting from the growth model. Successfully modeling the liquid-skin instabilities and accurately predicting the type and frequency of induced defects are daunting tasks. Calculating how the different structural defects influence a MWCNT's mechanical strength is also very challenging. A possible solution is to model a metastable catalyst to be oscillating between liquid and solid forms, with the time constants determined by the environment and the catalyst size. The produced MWCNTs should then be modeled as a series of high-quality segments joined by poor-quality nodes, the lengths of these parts being related to the time constants of liquid and solid forms. It would be interesting to study if such a simple model can reproduce the strongly nonlinear, diameter-dependent change in elastic modulus.

Acknowledgment. We thank A. Fonseca and J. B. Nagy, Facultés Universitaires Notre-Dame de la Paix, for providing the nanotube samples; S. Delpeux, T. Cacciaguerra, and F. Béguin, Centre National de la Recherche Scientifique, for the heat treatment; B. Dwir, EPFL, for providing the GaAs structures; G. Beney, EPFL, for polishing these structures; and J. D. Renton, University of Cambridge, for discussions on anisotropic elasticity. We also thank the Centre Interdisciplinaire de Microscopie Electronique (CIME) at EPFL for access to electron microscopes and technical support. G. A. D. Briggs thanks the Engineering and Physical Sciences Research Council (EPSRC) for a Professorial Research Fellowship (GR/S15808/01). This work was supported by the National Center of Competence in Research (NCCR) "Nanoscale Science" of the Swiss National Science Foundation.

References

(1) Queries at the Web of Science (http://www.isiknowledge.com) showed that the following numbers of articles have been published on the topic of "'chemical vapo*r deposition' AND 'carbon nanotube*'", in the publication years given in parantheses: 275 (2002), 398 (2003), 440 (2004), 489 (2005), and 608 (2006). The topics "'arc discharge' AND 'carbon nanotube*'" and "'laser ablation' AND 'carbon nanotube*'" returned 360 and 199 publications, respectively, for the whole five-year period. The majority of the counted publications are concerned with aspects other than the growth process, but the numbers are arguably good reflections of the availability and the popularity of CVD-grown CNTs.
(2) Couteau, E.; Hernadi, K.; Seo, J. W.; Thien-Nga, L.; Mikó, Cs.; Gaál, R.; Forró, L. *Chem. Phys. Lett.* **2003**, *378*, 9−17.
(3) Li, Y.-L.; Kinloch, I. A.; Windle, A. H. *Science* **2004**, *304*, 276−278.
(4) Magrez, A.; Seo, J. W.; Mikó, Cs.; Hernádi, K.; Forró, L. *J. Phys. Chem. B* **2005**, *109*, 10087−10091.
(5) Magrez, A.; Seo, J. W.; Kuznetsov, V. L.; Forró, L. *Angew. Chem. Int. Ed.* **2007**, *46*, 441−444.
(6) Dai, H. Nanotube Growth and Characterization. In *Carbon Nanotubes: Synthesis, Structure, Properties, and Applications*; Dresselhaus, M. S., Dresselhaus, G., Avouris, P., Eds.; Springer: Heidelberg, Germany, 2001; pp 29−54.
(7) Wagner, R. S.; Ellis, W. C. *Appl. Phys. Lett.* **1964**, *4*, 89−90.
(8) Dupuis, A.-C. *Prog. Mater. Sci.* **2005**, *50*, 929−961.
(9) Homma, Y.; Kobayashi, Y.; Ogino, T.; Takagi, D.; Ito, R.; Jung, Y. J.; Ajayan, P. M. *J. Phys. Chem. B* **2003**, *107*, 12161−12164.
(10) Buffat, Ph.; Borel, J.-P. *Phys. Rev. A* **1976**, *13*, 2287−2298.
(11) Ding, F.; Bolton, K.; Rosén, A. *J. Vac. Sci. Technol., A* **2004**, *22*, 1471−1476.
(12) Harutyunyan, A. R.; Tokune, T.; Mora, E. *Appl. Phys. Lett.* **2005**, *87*, 051919.
(13) Nanda, K. K.; Sahu, S. N.; Behera, S. N. *Phys. Rev. A* **2002**, *66*, 013208.
(14) Ding, F.; Rosén, A.; Curtarolo, S.; Bolton, K. *Appl. Phys. Lett.* **2006**, *88*, 133110.
(15) Kukovitsky, E. F.; L'vov, S. G.; Sainov, N. A. *Chem. Phys. Lett.* **2000**, *317*, 65−70.
(16) Chadderton, L. T.; Chen, Y. *J. Cryst. Growth* **2002**, *240*, 164−169.
(17) Kukovitsky, E. F.; L'vov, S. G.; Sainov, N. A.; Shustov, V. A.; Chernozatonskii, L. A. *Chem. Phys. Lett.* **2002**, *355*, 497−503.
(18) Bartsch, K.; Leonhardt, A. *Carbon* **2004**, *42*, 1731−1736.
(19) Bartsch, K.; Biedermann, K.; Gemming, T.; Leonhardt, A. *J. Appl. Phys.* **2005**, *97*, 114301.
(20) Treacy, M. M. J.; Ebbesen, T. W.; Gibson, J. M. *Nature* **1996**, *381*, 678−680.
(21) Wong, E. W.; Sheehan, P. E.; Lieber, C. M. *Science* **1997**, *277*, 1971−1975.
(22) Falvo, M. R.; Clary, G. J.; Taylor, R. M., II; Chi, V.; Brooks, F. P., Jr.; Washburn, S.; Superfine, R. *Nature* **1997**, *389*, 582−584.
(23) Salvetat, J.-P.; Kulik, A. J.; Bonard, J.-M.; Briggs, G. A. D.; Stöckli, T.; Méténier, K.; Bonnamy, S.; Béguin, F.; Burnham, N. A.; Forró, L. *Adv. Mater.* **1999**, *11*, 161−165.
(24) Lukić, B.; Seo, J. W.; Couteau, E.; Lee, K.; Gradečak, S.; Berkecz, R.; Hernadi, K.; Delpeux, S.; Cacciaguerra, T.; Béguin, F.; Fonseca, A.; Nagy, J. B.; Csányi, G.; Kis, A.; Kulik, A. J.; Forró, L. *Appl. Phys. A* **2005**, *80*, 695−700.
(25) Lukić, B.; Seo, J. W.; Bacsa, R. R.; Delpeux, S.; Béguin, F.; Bister, G.; Fonseca, A.; Nagy, J. B.; Kis, A.; Jeney, S.; Kulik, A. J.; Forró, L. *Nano Lett.* **2005**, *5*, 2074−2077.
(26) Salvetat, J.-P.; Briggs, G. A. D.; Bonard, J.-M.; Bacsa, R. R.; Kulik, A. J.; Stöckli, T.; Burnham, N. A.; Forró, L. *Phys. Rev. Lett.* **1999**, *82*, 944−947.
(27) Gere, J. M.; Timoshenko, S. P. *Mechanics of Materials*, 3rd ed.; PWS-KENT: Boston, 1990.
(28) Yamamoto, K.; Akita, S.; Nakayama, Y. *J. Phys. D* **1998**, *31*, L34−L36.
(29) Cappella, B.; Dietler, G. *Surf. Sci. Rep.* **1999**, *34*, 1−104.
(30) Cannara, R. J.; Brukman, M. J.; Carpick, R. W. *Rev. Sci. Instrum.* **2005**, *76*, 053706.
(31) Kwon, J.; Hong, J.; Kim, Y.-S.; Lee, D.-Y.; Lee, K.; Lee, S.-M.; Park, S.-I. *Rev. Sci. Instrum.* **2003**, *74*, 4378−4383.
(32) Cantilever length: 85 μm; tip height: 5 μm; cantilever spring constant: 0.74 N/m; mounting angle: 12°.
(33) Overney, R. M.; Takano, H.; Fujihira, M. *Phys. Rev. Lett.* **1994**, *72*, 3546−3549.
(34) Hernadi, K.; Fonseca, A.; Nagy, J. B.; Bernaerts, D.; Fudala, A.; Lucas, A. A. *Zeolites* **1996**, *17*, 416−423.
(35) Chang, T.; Gao, H. *J. Mech. Phys. Solids* **2003**, *51*, 1059−1074.
(36) Wang, L.; Zheng, Q.; Liu, J. Z.; Jiang, Q. *Phys. Rev. Lett.* **2005**, *95*, 105501.
(37) Poncharal, Ph.; Wang, Z. L.; Ugarte, D.; de Heer, W. A. *Science* **1999**, *283*, 1513−1516.
(38) Akita, S.; Sawaya, S.; Nakayama, Y. Mechanical Vibrations of Carbon Nanotube Cantilevers. *Abstract Book*, International Conference on Nanoscience and Technology (ICN+T), Basel, Switzerland, Jul 30−Aug 4, 2006; P1263, p 335.
(39) Renton, J. D. *Elastic Beams and Frames*; Horwood: Chichester, U.K., 2002.
(40) Vanfleet, R. R.; Mochel, J. M. *Surf. Sci.* **1995**, *341*, 40−50.
(41) Puretzky, A. A.; Geohegan, D. B.; Jesse, S.; Ivanov, I. N.; Eres, G. *Appl. Phys. A* **2005**, *81*, 223−240.
(42) Helveg, S.; López-Cartes, C.; Sehested, J.; Hansen, P. L.; Clausen, B. S.; Rostrup-Nielsen, J. R.; Abild-Pedersen, F.; Nørskov, J. K. *Nature* **2004**, *427*, 426−429.

NL070502B